

Direct detection of Higgs–portal dark matter at the LHC

Abdelhak Djouadi^{a,b,*}, Adam Falkowski^{a,†}, Yann Mambrini^{a,‡} and Jérémie Quevillon^{a,§}

^a *Laboratoire de Physique Théorique, Université Paris-Sud, F-91405 Orsay, France.*

^b *CERN, CH-1211, Geneva 23, Switzerland.*

We consider the process in which a Higgs particle is produced in association with jets and show that monojet searches at the LHC already provide interesting constraints on the invisible decays of a 125 GeV Higgs boson. Using the latest monojet search performed by the CMS collaboration with 4.7 fb^{-1} of data, we set the 90% confidence level limit on the invisible Higgs decay rate to be less than the total Higgs rate in the Standard Model. This limit could be significantly improved when more data at higher center of mass energies are collected, provided systematic errors on the Standard Model contribution to the monojet background can be reduced. In the context of Higgs portal models of dark matter, we then discuss how the LHC limits on the invisible Higgs branching fraction impose strong constraints on the dark matter scattering cross section on nucleons probed in direct detection experiments.

Introduction

The latest results on Higgs particle searches at the LHC and the Tevatron show tantalizing hints of a signal of a particle with a mass around $M_H = 125 \text{ GeV}$ [1]. The most pronounced signal is observed in the $\gamma\gamma$ final state, while the results from other available search channels are in a reasonable agreement with the Higgs boson interpretation within the Standard Model (SM) [2, 3]. It is plausible that data from the ongoing 8 TeV run of the LHC will firmly establish the existence of a Higgs boson. Even if that is the case, the Higgs particle may have other decay channels that are not predicted by the SM. Determining or constraining non-standard Higgs boson decays will provide a vital input to model building in the context of physics beyond the SM.

A very interesting possibility that is often discussed is a Higgs boson decaying into stable particles that do not interact with the detector, the so-called (fully or partly) invisible Higgs. Common examples where Higgs particles can have invisible decay modes include decays into the lightest supersymmetric particle [4] or decays into heavy neutrinos in the SM extended by a fourth generation of fermions [5]. In a wider context, the Higgs boson could be coupled to the particle that constitutes all or part of the dark matter in the universe. In these so-called *Higgs portal* models [6] the Higgs boson is the key mediator in the process of dark matter annihilation and scattering, providing an intimate link between Higgs hunting in collider experiments and the direct search for dark matter particles in their elastic scattering on nucleons. In fact, the present LHC Higgs search results, combined with the constraints on the direct detection cross section from the XENON experiment [7], severely constrain the

Higgs couplings to dark matter particles and have strong consequences on invisible Higgs decay modes for scalar, fermionic or vectorial dark matter candidates [8].

At the LHC, the main channel for producing a relatively light SM–like Higgs boson is the gluon–gluon fusion (ggF) mechanism. At leading order (LO), the process proceeds through a heavy top quark loop, leading to a single Higgs boson in the final state, $gg \rightarrow H$ [9]. A next-to-leading order (NLO) in perturbative QCD, an additional jet can be emitted by the initial gluons or the internal heavy quarks, leading to $gg \rightarrow Hg$ final states [10] (additional contributions are also provided by the $gg \rightarrow Hq$ process). As the QCD corrections turn out to be quite large, the rate for $H+1$ jet is not much smaller than the rate for $H+0$ jet. The next-to-next-to-leading order (NNLO) QCD corrections [11, 12], besides significantly increasing the $H+0$ and $H+1$ jet rates, lead to $H+2$ jet events. The latter event topology also occurs at LO in two other Higgs production mechanisms: vector boson fusion (VBF) $qq \rightarrow Hqq$ and Higgs–strahlung (VH) $q\bar{q} \rightarrow HW/HZ \rightarrow Hq\bar{q}$ which have rather distinct kinematical features compared to the gluon fusion process; for a review, see Ref. [4].

Hence, if the Higgs boson is coupled to invisible particles, it may recoil against hard QCD radiation, leading to monojet events at the LHC. In this note, we show that the monojet signature carries a good potential to constrain the invisible decay width of a 125 GeV Higgs boson. In a model independent fashion, constraints can be placed on the Higgs invisible rates $R_{\text{inv}}^{\text{ggF}}$ and $R_{\text{inv}}^{\text{VBF}}$ defined as

$$\begin{aligned} R_{\text{inv}}^{\text{ggF}} &= \frac{\sigma(gg \rightarrow H) \times \text{BR}(H \rightarrow \text{inv.})}{\sigma(gg \rightarrow H)_{\text{SM}}}, \\ R_{\text{inv}}^{\text{VBF}} &= \frac{\sigma(qq \rightarrow Hqq) \times \text{BR}(H \rightarrow \text{inv.})}{\sigma(qq \rightarrow Hqq)_{\text{SM}}}. \end{aligned} \quad (1)$$

We will argue that the recent monojet search performed by the CMS collaboration [13] is sensitive to R_{inv} close to unity. It has been shown that if the total production rate of a 125 GeV Higgs boson is close to the SM one then,

*Electronic address: abdelhak.djouadi@th.u-psud.fr

†Electronic address: adam.falkowski@th.u-psud.fr

‡Electronic address: yann.mambrini@th.u-psud.fr

§Electronic address: jeremie.quevillon@th.u-psud.fr

based on the combined data from the *visible* Higgs decay channels, $\text{BR}(H \rightarrow \text{inv.}) > 0.4$ is already disfavored [3, 14]. However, in models beyond the SM, the Higgs production rate may well be enhanced (for instance, in the presence of additional heavy quarks that couple to the Higgs boson), in which case the constraints from monojet searches discussed here become non-trivial. In this sense, our approach is complementary to that adopted in Refs. [3, 14] (see also Ref. [15]) in which the invisible branching fraction is indirectly constrained via visible Higgs decays.

In the next step, we discuss the connection between the Higgs invisible branching fraction and the direct dark matter detection cross section. We work in the context of Higgs portal models and consider the cases of scalar, fermionic and vectorial dark matter particles (that we generically denote by χ) coupled to the Higgs boson. To keep our discussion more general, the Higgs- $\chi\chi$ couplings are not fixed by the requirement of obtaining the correct relic density from thermal history¹. In each case, the LHC constraint $\text{BR}(H \rightarrow \text{inv.})$ can be translated into a constraint on the Higgs boson couplings to the dark matter particles. We will show that these constraints are competitive with those derived from the XENON bounds on the dark matter scattering cross section on nucleons². We discuss how future results from invisible Higgs searches at the LHC and from direct detection experiments will be complementary in exploring the parameter space of Higgs portal models.

The rest of this letter is organized as follows. In the next section, we summarize our analysis of invisible Higgs plus jet production at the LHC. We estimate the sensitivity to the invisible Higgs rate of the recent CMS monojet search using 4.7 fb^{-1} of data at $\sqrt{s} = 7 \text{ TeV}$, extending previous analyses [17] based on the 1 fb^{-1} ATLAS monojet search [18]. In the following section, we discuss the implications for Higgs portal dark matter models and the complementarity between dark matter direct detection at the LHC and in XENON. In the last section we present short conclusions.

Monojet constraints on the invisible width

In this section we estimate the sensitivity of current monojet searches at the LHC to a Higgs particles that decays invisibly. We rely on the search for monojets performed by the CMS collaboration which makes use of 4.7 fb^{-1} of data at 7 TeV center of mass energy [13]. The ba-

sic selection requirements used by the CMS experiment for such a topology are as follows:

- at least 1 jet with $p_T^j > 110 \text{ GeV}$ and $|\eta^j| < 2.4$;
- at most 2 jets with $p_T^j > 30 \text{ GeV}$;
- no isolated leptons;
- missing transverse momentum $p_T^{\text{miss}} \geq 200 \text{ GeV}$.

A second jet with p_T^j above 30 GeV is allowed provided it is not back-to-back with the leading one, $\Delta\phi(j_1, j_2) < 2.5$. Incidentally, this is advantageous from the point of view of invisible Higgs searches, as Higgs production at the LHC is often accompanied by more than one jet; vetoing the second jet would reduce the signal acceptance by a factor of ~ 2 . The CMS collaboration quotes the event yields for 5 different cuts on the missing transverse momentum p_T^{miss} between 200 and 400 GeV. These are largely dominated by the SM backgrounds, namely Z +jets, where the Z boson decays invisibly, and W +jets, where the W boson decays leptonically and the charged lepton is not reconstructed. In particular, with 4.7 fb^{-1} data, the CMS collaboration estimates the background to be 24535 (1224) events for $p_T^{\text{miss}} > 200$ (350) GeV, with an uncertainty that is below the 10% level.

A Higgs boson produced with a significant transverse momentum and decaying to invisible particles can also lead to the topology that is targeted by monojet searches. In Fig.1, we show the fraction of Higgs events produced at the parton level in the ggF and VBF processes with p_T^j above a given threshold, assuming $M_H = 125 \text{ GeV}$. One observes that about 1% (0.1%) of ggF events are produced with $p_T^j > 200$ (350) GeV which, assuming the SM production cross section, corresponds to about 750 (75) events in 5 fb^{-1} data at the $\sqrt{s} = 7 \text{ TeV}$ LHC. For the VBF and VH production processes, that fraction is larger by a factor of ~ 3 . These numbers are comparable to the uncertainty on the SM monojet background quoted by the CMS collaboration. This suggests that if an invisible Higgs boson is produced with rates that are comparable or larger than the total rate of a SM-like Higgs boson, the monojet searches may already provide interesting constraints.

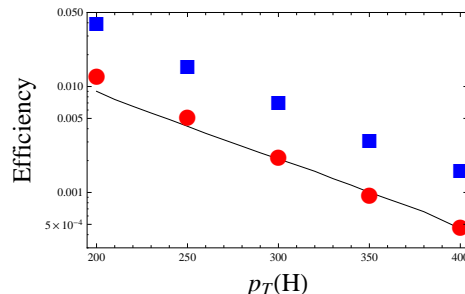


FIG. 1: The fraction of events with Higgs transverse momentum above a given threshold for the ggF (red circles) and VBF (blue squares) production modes. The distributions were obtained at NLO using the program POWHEG [19]. In the case of ggF, the simulations included the finite quark mass effects [20], and we find good agreement with the NNLO distribution obtained using the program HRes [12] (black line).

¹ Instead, we assume that one of the multiple possible processes (e.g. co-annihilation, non-thermal production, s -channel poles of particles from another sector) could arrange that the dark matter relic abundance is consistent with cosmological observations.

² We note that the process $gg \rightarrow H \rightarrow \chi\chi$ for dark matter χ production at the LHC is an important component of the (crossed) process for dark matter scattering on nucleons, $g\chi \rightarrow g\chi$ [16].

In order to estimate the sensitivity of the CMS monojet search to the invisible Higgs signal, we generated the $pp \rightarrow H + \text{jets} \rightarrow \text{invisible} + \text{jets}$ process. We used the program POWHEG [19, 20] for the ggF and VBF channels at the parton level, and Madgraph 5 [21] for the VH channels. Showering and hadronisation was performed using Pythia 6 [22] and Delphes 1.9 [23] was employed to simulate the CMS detector response. We imposed the analysis cuts listed above on the simulated events so as to find the signal efficiency. As a cross-check, we passed $(Z \rightarrow \nu\nu) + \text{jets}$ background events through the same simulation chain, obtaining efficiencies consistent within 15% with the data-driven estimates of that background provided by CMS.

The signal event yield depends on the cross section in each Higgs production channel and on the Higgs branching fraction into invisible final states. Thus, strictly speaking, the quantities that are being constrained by the CMS search are³ $R_{\text{inv}}^{\text{ggF}}$ and $R_{\text{inv}}^{\text{VBF}}$ that are given in Eq. (1). Currently available data do not allow us to independently constrain $R_{\text{inv}}^{\text{ggF}}$ and $R_{\text{inv}}^{\text{VBF}}$. Thus, for the sake of setting limits, we assume that the proportions of ggF, VBF and VH rates are the same as in the SM, and we take the inclusive cross sections to be $\sigma(gg \rightarrow H)_{\text{SM}} = 15.3$ pb, $\sigma(qq \rightarrow Hqq)_{\text{SM}} = 1.2$ pb and $\sigma(q\bar{q} \rightarrow HV)_{\text{SM}} = 0.9$ pb [24]. With this assumption, after the analysis cuts, the signal receives about 30% contribution from the VBF and VH production modes, and the rest from ggF; thus one constrains the combination $R_{\text{inv}}^{\text{pp}} \approx \frac{2}{3} R_{\text{inv}}^{\text{ggF}} + \frac{1}{3} R_{\text{inv}}^{\text{VBF}}$.

Our results are presented in Table I. We display the predicted event yield N_{inv} in the ggF and VBF channels for each cut on p_T^{miss} reported by the CMS collaboration. Comparing it to the 1σ background uncertainty⁴ listed by CMS, we derive the expected 95% confidence level (CL) limit on R_{inv} . We find the best expected limit is at the level of $R_{\text{inv}} \leq 2$ for the $p_T^j \geq 250$ and 300 GeV cuts. The observed limit is better than the expected one in most cases, thanks to a $\sim 1\sigma$ downward fluctuation of the SM background. We find that the best limit corresponds to the $p_T^j \geq 250$ GeV cut, which yields the constraint $R_{\text{inv}} \leq 1.3$ (1.0) at 95% (90%) CL. Finally, we can

p_T^{miss}	$N_{\text{inv}}^{\text{ggF}}$	$N_{\text{inv}}^{\text{VBF}}$	ΔN_{Bkg}	$R_{\text{inv}}^{\text{exp}}$	$R_{\text{inv}}^{\text{obs}}$
200	630	260	~ 1200	2.6	1.8
250	250	110	~ 380	2.0	1.3
300	110	50	~ 170	2.1	2.2
350	46	25	101	2.8	1.6
400	22	13	~ 70	3.8	2.3

TABLE I: Predicted event yields N_{inv} , the 1σ background uncertainty ΔN_{Bkg} , and the expected and observed 95% CL limits on the invisible Higgs rate R_{inv} for each reported missing energy cut of the CMS monojet search. The event yields are given separately for the ggF and VBF+VH production modes, assuming the SM Higgs production cross sections in these channels.

separately constrain $R_{\text{inv}}^{\text{ggF}}$ and $R_{\text{inv}}^{\text{VBF}}$ assuming only *one* Higgs production mode is present. Again the best limit is found using the CMS results for $p_T^j \geq 250$ GeV, and we find $R_{\text{inv}}^{\text{ggF}} \leq 1.9$ (when VBF is absent) or $R_{\text{inv}}^{\text{VBF}} \leq 4.3$ (when ggF is absent) at 95% CL.

Assuming Higgs produced with the SM cross section, the direct bounds from monojet searches do not yet constrain the invisible branching fraction. However, as discussed previously, in many models beyond the SM the Higgs production rate can be significantly enhanced, especially in the gluon fusion channel, in which case the current monojets bounds become non-trivial. In any case we should note that the sensitivity of monojet searches to invisible Higgs turns out to be much better than expected. Indeed, early studies [25], focusing mainly on the VBF production channel, concluded that observation of invisible Higgs decays was only possible at the highest LHC energy, $\sqrt{s} = 14$ TeV, and with more than 10 fb^{-1} data. Bounds on invisible Higgs based on the 1 fb^{-1} monojet search in ATLAS [18] were studied in Ref. [17], where a weaker limit of $R_{\text{inv}}^{\text{ggh}} \lesssim 4$ was obtained for $M_h \sim 125$ GeV. In contrast, our analysis shows that with 5 fb^{-1} data at 7 TeV, the LHC is already sensitive to R_{inv} of order 1. Note also that monojet searches are sensitive mostly to the ggF mode, thus they can also probe invisible Higgs in models where the Higgs couplings to the W, Z bosons are reduced, providing complementary information to invisible Higgs searches targeting the VBF mode.

We expect the bounds on the invisible Higgs width to be improved in the ongoing 8 TeV run. To make an estimate of the future sensitivity, we assume the error on the $Z \rightarrow \nu\nu + \text{jets}$ background contribution will be dominated, as in the current run, by the statistics of the $Z \rightarrow \mu\mu + \text{jets}$ control sample. We also (arbitrarily) assume the systematic error on the $W \rightarrow \ell\nu + \text{jets}$ background contribution will be brought down to 5%. Taking into account the increased cross section⁵ and selection efficiency for the

³ Assuming custodial symmetry, $R_{\text{inv}}^{\text{VH}} = R_{\text{inv}}^{\text{VBF}}$.

⁴ The CMS collaboration quotes the estimate of each important background for every p_T^{miss} cut but the errors on those estimates are given only for the $p_T^j \geq 350$ GeV cut. In the remaining cases, we estimated the uncertainty assuming that the error on the $Z \rightarrow \nu\nu + \text{jets}$ background is dominated by statistics of the $Z \rightarrow \ell\ell + \text{jets}$ control sample, while the error on the $W \rightarrow \ell\nu + \text{jets}$ background is systematic and equals 11.3%. The remaining (sub-leading) backgrounds are assigned 100% uncertainty. Note that we did not consider the theoretical uncertainties on the cross sections [24] and the efficiencies of the p_T cuts which, although significant, are currently smaller than the experimental ones.

⁵ The inclusive cross sections at $\sqrt{s} = 8$ TeV are found to be 20.1, 1.6 and 1.1 pb for, respectively, ggF, VBF and VH.

signal and the V +jets backgrounds, we estimate the expected bound to be $R_{\text{inv}}^{\text{exp}} < 0.9$ at 95%CL with 15 fb^{-1} at $\sqrt{s}=8 \text{ TeV}$. Obviously, this is just a crude estimate, as it crucially depends on experiments' ability to control systematic errors on the V +jets backgrounds.

Invisible branching fraction and direct detection

If the invisible particle into which the Higgs boson decays is a constituent of dark matter in the universe, the Higgs coupling to dark matter can be probed not only at the LHC but also in direct detection experiments. In this section, we discuss the complementarity of these two direct detection methods. We consider generic Higgs-portal scenarios in which the dark matter particle is a real scalar, a real vector, or a Majorana fermion, $\chi = S, V, f$ [8, 26]. The relevant terms in the effective Lagrangian in each of these cases are

$$\begin{aligned}\Delta\mathcal{L}_S &= -\frac{1}{2}m_S^2 S^2 - \frac{1}{4}\lambda_S S^4 - \frac{1}{4}\lambda_{hSS} H^\dagger H S^2, \\ \Delta\mathcal{L}_V &= \frac{1}{2}m_V^2 V_\mu V^\mu + \frac{1}{4}\lambda_V (V_\mu V^\mu)^2 + \frac{1}{4}\lambda_{hVV} H^\dagger H V_\mu V^\mu, \\ \Delta\mathcal{L}_f &= -\frac{1}{2}m_f \bar{f} f - \frac{1}{4}\frac{\lambda_{hff}}{\Lambda} H^\dagger H \bar{f} f + \text{h.c.} \end{aligned} \quad (2)$$

The partial Higgs decay width into dark matter $\Gamma(H \rightarrow \chi\chi)$ and the spin-independent χ -proton elastic cross section $\sigma_{\chi p}^{\text{SI}}$ can be easily calculated in terms of the parameters of the Lagrangian, and we refer to Ref. [8] for complete expressions. For the present purpose, it is important that both $\Gamma(H \rightarrow \chi\chi)$ and $\sigma_{\chi p}^{\text{SI}}$ are proportional to $\lambda_{H\chi\chi}^2$; therefore, the ratio $r_\chi = \Gamma(H \rightarrow \chi\chi)/\sigma_{\chi p}^{\text{SI}}$ depends only on the dark matter mass M_χ and known masses and couplings (throughout, we assume the Higgs mass be $M_H = 125 \text{ GeV}$). This allows us to relate the invisible Higgs branching fraction to the direct detection cross section:

$$\text{BR}_\chi^{\text{inv}} \equiv \frac{\Gamma(H \rightarrow \chi\chi)}{\Gamma_H^{\text{SM}} + \Gamma(H \rightarrow \chi\chi)} = \frac{\sigma_{\chi p}^{\text{SI}}}{\Gamma_H^{\text{SM}}/r_\chi + \sigma_{\chi p}^{\text{SI}}} \quad (3)$$

with Γ_H^{SM} the total decay width into all particles in the SM. For a given M_χ , the above formula connects the invisible branching fraction probed at the LHC to the dark matter-nucleon scattering cross section probed by XENON100. For $m_p \ll M_\chi \ll \frac{1}{2}M_H$, and assuming the visible decay width equals to the SM total width $\Gamma_H^{\text{SM}} = 4.0 \text{ MeV}$ [27], one can write down the approximate relations in the three cases that we are considering,

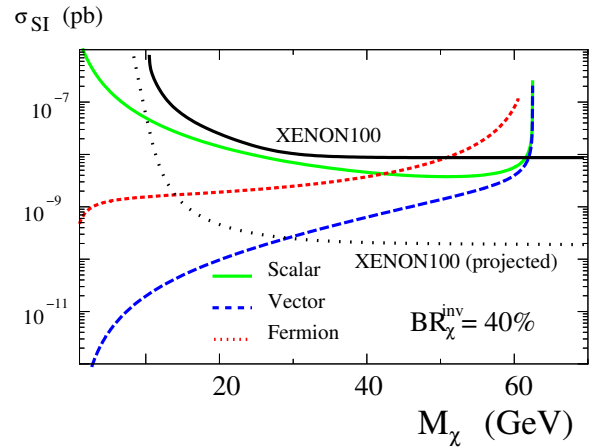
$$\begin{aligned}\text{BR}_S^{\text{inv}} &\simeq \frac{\left(\frac{\sigma_{Sp}^{\text{SI}}}{10^{-9}\text{pb}}\right)}{400 \left(\frac{10 \text{ GeV}}{M_S}\right)^2 + \left(\frac{\sigma_{Sp}^{\text{SI}}}{10^{-9}\text{pb}}\right)} \\ \text{BR}_V^{\text{inv}} &\simeq \frac{\left(\frac{\sigma_{Vp}^{\text{SI}}}{10^{-9}\text{pb}}\right)}{4 \times 10^{-2} \left(\frac{M_V}{10 \text{ GeV}}\right)^2 + \left(\frac{\sigma_{Vp}^{\text{SI}}}{10^{-9}\text{pb}}\right)}\end{aligned}$$

$$\text{BR}_f^{\text{inv}} \simeq \frac{\left(\frac{\sigma_{fp}^{\text{SI}}}{10^{-9}\text{pb}}\right)}{3.47 + \left(\frac{\sigma_{fp}^{\text{SI}}}{10^{-9}\text{pb}}\right)} \quad (4)$$

Thus, for a given mass of dark matter, an upper bound on the Higgs invisible branching fraction implies an upper bound on the dark matter scattering cross section on nucleons. In Fig. 2 we show the maximum allowed values of the scattering cross section, assuming the 40% bound on $\text{BR}_\chi^{\text{inv}}$ advocated in Ref. [3]. Clearly, the relation between the invisible branching fraction and the direct detection cross section strongly depends on the spinorial nature of the dark matter particle, in particular, the strongest (weakest) bound is derived in the vectorial (scalar) case.

In all cases, the derived bounds on $\sigma_{\chi p}^{\text{SI}}$ are stronger than the direct one from XENON100 in the entire range where $M_\chi \ll \frac{1}{2}M_H$. In other words, the LHC is currently the most sensitive dark matter detection apparatus, at least in the context of simple Higgs-portal models (even more so if χ is a pseudoscalar, as in [29]). This conclusion does not rely on the assumption that the present abundance of χ is a thermal relic fulfilling the WMAP constraint of $\Omega_{DM} = 0.226$ [28], and would only be stronger if χ constitutes only a fraction of dark matter in the universe. We also compared the bounds to the projected future sensitivity of the XENON100 experiment (corresponding to 60,000 kg-d, 5-30 keV and 45% efficiency).

Of course, for $M_\chi > \frac{1}{2}M_H$, the Higgs boson cannot decay into dark matter⁶, in which case the LHC cannot compete with the XENON bounds.



⁶ In this case, one should consider the pair production of dark matter particles through virtual Higgs boson exchange, $pp \rightarrow H^* X \rightarrow \chi\chi X$. The rates are expected to be rather small [8, 30].

FIG. 2: Bounds on the spin-independent direct detection cross section $\sigma_{\chi p}^{\text{SI}}$ in Higgs portal models derived for $M_H = 125$ GeV and the invisible branching fraction of 40 % (colored lines). The curves take into account the full M_χ dependence, without using the approximation in Eq. 4. For comparison, we plot the current and future direct bounds from the XENON experiment (black lines).

Conclusions

We have shown that monojet searches at the LHC already provide interesting limits on invisible Higgs decays, constraining the invisible rate to be less than the total SM Higgs production rate at the 90% CL. This constrains the invisible branching fraction in models where the Higgs production cross section is enhanced, for example by the presence of additional heavy chiral quarks. Monojets searches are sensitive mostly to the gluon–gluon fusion production mode and, thus, they can also probe invisible Higgs decays in models where the Higgs coupling to the electroweak gauge bosons is suppressed. The limits could be significantly improved when more data at higher center of mass energies are collected, provided systematic errors on the Standard Model contribution to the monojet background can be reduced. We expect that the monojet data which will be collected in the ongoing 8 TeV LHC

run will place non-trivial constraints on the Higgs invisible branching fraction, even if the Higgs production rate is SM-like.

We also analyzed in a model-independent way the interplay between the invisible Higgs branching fraction and the dark matter scattering cross section on nucleons, in the context of effective Higgs portal models. The limit $\text{BR}_{\text{inv}} < 0.4$, suggested by the combination of Higgs data in the visible channels, implies a limit on the direct detection cross section that is stronger than the current bounds from XENON100, for scalar, fermionic, and vectorial dark matter alike. Hence, in the context of Higgs-portal models, the LHC is currently the most sensitive dark matter detection apparatus.

Acknowledgements: The authors would like to thank J. Baglio, E. Bagnaschi, E. Bragina, C. Grojean, P. Boucaud, and T. Volansky as well as the Magic Monday Journal Club for discussions. This work was supported by the French ANR TAPDMS *ANR-09-JCJC-0146* and the Spanish MICINN Consolider-Ingenio 2010 Programme under grant Multi- Dark *CSD2009-00064*. A.D. thanks the CERN TH unit for hospitality and support.

-
- [1] G. Aad *et al.* [ATLAS Collaboration], Phys. Lett. B **710** (2012) 49 [arXiv:1202.1408 [hep-ex]]; S. Chatrchyan *et al.* [CMS Collaboration], Phys. Lett. B **710** (2012) 26 [arXiv:1202.1488 [hep-ex]]; [TEVNPWG, CDF and D0 Collaborations], arXiv:1203.3774 [hep-ex].
 - [2] D. Carmi, A. Falkowski, E. Kuflik and T. Volansky, arXiv:1202.3144 [hep-ph]; A. Azatov, R. Contino and J. Galloway, arXiv:1202.3415 [hep-ph]; J. R. Espinosa, C. Grojean, M. Muhlleitner and M. Trott, arXiv:1202.3697 [hep-ph]; J. Ellis and T. You, arXiv:1204.0464 [hep-ph].
 - [3] P. P. Giardino, K. Kannike, M. Raidal and A. Strumia, arXiv:1203.4254 [hep-ph].
 - [4] For reviews on Higgs physics, see e.g. A. Djouadi, Phys. Rept. **457** (2008) 1 [hep-ph/0503172]; Phys. Rept. **459** (2008) 1 [hep-ph/0503173].
 - [5] Note that in view of the recent LHC data, a perturbative SM with a 4th generation fermions is excluded; see A. Djouadi and A. Lenz, arXiv:1204.1252 [hep-ph]; E. Kuflik, Y. Nir and T. Volansky, arXiv:1204.1975 [hep-ph].
 - [6] V. Silveira, A. Zee, Phys. Lett. **B161**, 136 (1985); J. McDonald, Phys. Rev. **D50** (1994) 3637-3649; C. P. Burgess, M. Pospelov, T. ter Veldhuis, Nucl. Phys. **B619** (2001) 709-728 [hep-ph/0011335]; H. Davoudiasl, R. Kitano, T. Li and H. Murayama, Phys. Lett. B **609**, 117 (2005) [hep-ph/0405097]; B. Patt and F. Wilczek, hep-ph/0605188. S. Andreas, C. Arina, T. Hambye, F. -S. Ling, M. H. G. Tytgat, Phys. Rev. **D82** (2010) 043522 [arXiv:1003.2595 [hep-ph]]; M. Raidal, A. Strumia, Phys. Rev. **D84** (2011) 077701 [arXiv:1108.4903 [hep-ph]]; X. -G. He, J. Tandeau, Phys. Rev. **D84** (2011) 075018 [arXiv:1109.1277 [hep-ph]]. For review see e.g. Y. Mambrini, Phys. Rev. D **84** (2011) 115017 [arXiv:1108.0671 [hep-ph]]; arXiv:1112.0011 [hep-ph].
 - [7] E. Aprile *et al.* [XENON100 Collaboration], arXiv:1104.3121 and arXiv:1104.2549.
 - [8] A. Djouadi, O. Lebedev, Y. Mambrini and J. Quevillon, Phys. Lett. B **709** (2012) 65 [arXiv:1112.3299 [hep-ph]].
 - [9] H. Georgi, S. Glashow, M. Machacek, D. Nanopoulos, Phys. Rev. Lett. **40** (1978) 692.
 - [10] R.K. Ellis, I. Hinchliffe, M. Soldate and J.J. van der Bij, Nucl. Phys. **B297** (1988) 221; A. Djouadi, M. Spira and P.M. Zerwas, Phys. Lett. **B264** (1991) 440; S. Dawson, Nucl. Phys. **B359** (1991) 283; M. Spira, A. Djouadi, D. Graudenz and P. Zerwas, Nucl. Phys. **B453** (1995) 17.
 - [11] R. Harlander and W. Kilgore, Phys. Rev. Lett. **88** (2002) 201801; C. Anastasiou and K. Melnikov, Nucl. Phys. **B646** (2002) 220; V. Ravindran, J. Smith and W. van Neerven, Nucl. Phys. **B665** (2003) 325; S. Catani, D. de Florian, M. Grazzini, P. Nason, JHEP **0307** (2003) 028.
 - [12] D. de Florian, G. Ferrera, M. Grazzini and D. Tommasini, arXiv:1203.6321 [hep-ph].
 - [13] CMS-PAS-EXO-11-059, and the Winter 2012 update.
 - [14] V. Barger, M. Ishida and W. -Y. Keung, arXiv:1203.3456 [hep-ph].
 - [15] C. Englert, T. Plehn, M. Rauch, D. Zerwas and P. Zerwas, Phys. Lett. B **707** (2012) 512 [arXiv:1112.3007].
 - [16] M. Drees and M. Nojiri, Phys. Rev. **D48** (1993) 3483.
 - [17] Y. Bai, P. Draper and J. Shelton, arXiv:1112.4496 [hep-ph]. See also C. Englert, J. Jaeckel, E. Re and M. Spannowsky, Phys. Rev. D **85**, 035008 (2012) [arXiv:1111.1719 [hep-ph]].
 - [18] ATLAS-CONF-2011-096.
 - [19] S. Alioli, P. Nason, C. Oleari and E. Re, JHEP **0904** (2009) 002 [arXiv:0812.0578 [hep-ph]].
 - [20] E. Bagnaschi, G. Degrandi, P. Slavich and A. Vicini,

- JHEP **1202** (2012) 088 [arXiv:1111.2854 [hep-ph]].
- [21] J. Alwall, M. Herquet, F. Maltoni, O. Mattelaer and T. Stelzer, JHEP **1106** (2011) 128 [arXiv:1106.0522].
 - [22] T. Sjostrand, S. Mrenna and P. Z. Skands, JHEP **0605** (2006) 026 [hep-ph/0603175].
 - [23] S. Ovin, X. Rouby and V. Lemaitre, arXiv:0903.2225.
 - [24] J. Baglio and A. Djouadi, JHEP **1103** (2011) 055 [arXiv:1012.0530]; S. Dittmaier *et al.*, LHC Higgs cross section Working Group, arXiv:1101.0593.
 - [25] D. Choudhury and D. Roy, Phys. Lett. **B322** (1994) 368; O. Eboli and D. Zeppenfeld, Phys. Lett. **B495** (2000) 147; R. Godbole *et al.*, Phys. Lett. **B571** (2003) 184; H. Davoudiasl, T. Han and H. E. Logan, Phys. Rev. D **71** (2005) 115007; A. Alves, Phys. Rev. D **82**, 115021 (2010) [arXiv:1008.0016 [hep-ph]]; J. Kopp and Y. Tsai, Phys. Rev. D **85** (2012) 056011. For an ATLAS simulation, see D. Cavali *et al.*, hep-ph/0203056.
 - [26] T. Hambye and M. H. G. Tytgat, Phys. Lett. B **683**, 39 (2010) [arXiv:0907.1007 [hep-ph]]; S. Kanemura, S. Matsumoto, T. Nabeshima and N. Okada, Phys. Rev. D **82** (2010) 055026 [arXiv:1005.5651]; O. Lebedev, H. M. Lee and Y. Mambrini, Phys. Lett. B **707** (2012) 570 [arXiv:1111.4482 [hep-ph]]; J. F. Kamenik and C. Smith, arXiv:1201.4814 [hep-ph]; T. Nabeshima, arXiv:1202.2673.
 - [27] A. Djouadi, J. Kalinowski and M. Spira, Comput. Phys. Commun. **108** (1998) 56 [hep-ph/9704448].
 - [28] E. Komatsu *et al.* [WMAP Collaboration], Astrophys. J. Suppl. **192** (2011) 18 [arXiv:1001.4538].
 - [29] L. Lopez-Honorez, T. Schwetz and J. Zupan, arXiv:1203.2064 [hep-ph].
 - [30] Work in progress.